

Corrosion behavior of steel submitted to chloride and sulphate ions in simulated concrete pore solution



Guojian Liu, Yunsheng Zhang*, Ziwei Ni, Ran Huang

School of Materials Science and Engineering, Southeast University, Nanjing 21189, PR China

HIGHLIGHTS

- Corrosion behavior of steel submitted to chloride and/or sulphate is investigated.
- Chloride threshold value and corrosion threshold value of sulphate are obtained.
- The concomitant presence of chloride and sulphate leads to higher corrosion rate.

ARTICLE INFO

Article history:

Received 28 December 2015

Received in revised form 29 March 2016

Accepted 30 March 2016

Keywords:

Steel corrosion

Chloride threshold value

Sulphate ions

Electrochemical methods

ABSTRACT

Electrochemical measurements of open circuit potential, linear polarization and electrochemical impedance spectroscopy (EIS) were utilized to investigate the corrosion behavior and chloride threshold value (CTV) of reinforcing steels submitted to chloride and sulphate attack in simulated concrete pore solution in this study. Determination of corrosion initiation was made by combining half-cell potential (E_{corr}) with corrosion current density (I_{corr}) as well as EIS curves. Results showed that electrochemical measurements were effective in detecting corrosion behavior of steels. CTV of steels was 0.5–0.6 mol/L in simulated concrete pore solution contaminated by chloride ions while threshold value of steels submitted to sulphate ions was 0.2–0.3 mol/L. The concomitant presence of chloride and sulphate ions led to higher corrosion current density which indicated sulphate ions accelerated the corrosion of reinforcing steels in simulated concrete pore solution.

© 2016 Elsevier Ltd. All rights reserved.

1. Introduction

Steel reinforcement embedded in concrete normally maintains passive due to the thin iron oxides film which is attributed to the high alkaline environment of concrete. However, once the chloride content at the steel surface reaches a certain level, i.e. chloride threshold value (CTV), when oxygen and moisture in presence, active corrosion of steel is initiated [1–3]. Thus the CTV is defined as the chloride concentration at the depth of steel which triggers active or pitting corrosion. Premature deterioration of reinforced concrete structures induced by steel corrosion has become a serious durability problem throughout the world, leading to significant economic loss [4,5]. Numerous investigations [6–11] have been performed on ingress of aggressive ions and CTV, but reported values are rather scattered. For example, the chloride threshold value presented by total chloride in concrete ranged from 0.04 to 8.34% by weight of binder and from 0.07% to 1.16% expressed by free

chloride [12]. Besides, many reinforced concrete structures are exposed to harsh environment where concentrated chloride and sulphate ions coexist like in salt lake district or salinized soil district in northwest China [13]. Previously, a lot of emphasis has been placed on sulphate attack to concrete matrix [13–15] but few reports regarding influence of sulphate ions on steel corrosion are found.

Experiments performed in cement paste, mortar and concrete to investigate CTV of steels are time consuming and are greatly affected by many influencing factors such as cement type, concrete mix proportions, moisture content, temperature and blended materials [12,16], though it may reveal more pertinent results. Therefore many authors have performed studies on steel corrosion in simulated concrete pore solution, a saturated $\text{Ca}(\text{OH})_2$ solution in most cases [17,18]. Simulated concrete pore solutions not only reproduce chemical environment in concrete but also shorten the experiment period and provide significant results for cement-based materials.

In the present work, the corrosion behavior of steels submitted to chloride and/or sulphate ions in saturated $\text{Ca}(\text{OH})_2$ solution

* Corresponding author.

E-mail address: zhangys279@163.com (Y. Zhang).

(pH = 12.5) was investigated by employing open circuit potential (OCP), linear polarization (LP) and electrochemical impedance spectroscopy (EIS) methods. Corrosion initiation and the CTV were determined by combining half-cell potential (E_{corr}) with corrosion current density (I_{corr}) as well as EIS curves.

2. Experimental program

2.1. Specimen preparation and exposure conditions

Cylindrical steel specimens with a diameter of 16 mm and length of 10 mm were cut from HRB335 steel. The chemical composition of steel samples (by weight) was 0.20% C, 0.55% Si, 1.42% Mn, 0.028% S, 0.026% P and the balance of Fe. One cross-section surface was polished with grit paper to grade 1000 as exposure surface, degreased in acetone and then washed in distilled water. The remaining surface was sealed by epoxy resin. A copper wire was soldered to the other surface for electrochemical testing.

The saturated $Ca(OH)_2$ solution was prepared using distilled water, in which some insoluble $Ca(OH)_2$ remained. NaCl and/or Na_2SO_4 were added to saturated $Ca(OH)_2$ solution stepwise, 0.01 mol/L each day, as chloride and sulphate ions source. All chemical reagents applied in this study were analytical reagent grade.

2.2. Electrochemical techniques

All steel samples were immersed in saturated $Ca(OH)_2$ solution for ten days to obtain stable passive layer before experiment in order to simulate pre-passivated state in the concrete. Electrochemical tests were performed by using PARSTAT 2273 potentiostat/galvanostat immediately before adding new dosage of aggressive ions each day. With steel sample being working electrode, a saturated calomel electrode (SCE) and a platinum electrode were used as reference and counter electrodes, respectively. Half-cell potential, namely the E_{corr} , was with reference to SCE. The I_{corr} of steel reflecting corrosion rate was usually calculated by the LP method which is based on the Stern–Geary relationship [19] as in Eq. (1):

$$I_{corr} = \frac{\beta_a \beta_c}{2.303(\beta_a + \beta_c)} \frac{1}{R_p} = \frac{B}{R_p} \tag{1}$$

where I_{corr} is the corrosion current density, R_p the polarization resistance, B a constant related to β_a and β_c , the anodic and cathodic slopes of Tafel curve, respectively. The value of B is usually assumed to be from 26 mV to 52 mV [20]. The value of 26 mV was adopted in this study with the maximum error in the measurement a factor of 2. In this work, the R_p was obtained directly by built-in fitting software. EIS scan was carried out at the open-circuit potential with an AC signal of amplitude 10 mV and sweep frequency from 10 mHz to 100 kHz.

3. Results and discussion

3.1. Corrosion behavior in chloride contaminated condition

Three parallel steel samples labeled as #1, #2 and #3 are exposed to chloride added stepwise by 0.01 mol/L each day. The evolutions of E_{corr} are presented in Fig. 1. It can be found that the average E_{corr} of specimens after ten days of pre-passivation

is around -230 mV vs. SCE. With the additions of chloride, The E_{corr} decreases gradually and moves to negative values, which means a higher risk of corrosion. Then the E_{corr} drops dramatically when a certain content of chloride is added, indicating the breakdown of passive film and initiation of active corrosion. The CTV of steels can be inferred to be from 0.05 to 0.06 mol/L.

The evolutions of I_{corr} obtained from the LP and Eq. (1) are depicted in Fig. 2. With lower concentration of chloride, I_{corr} keeps a steady low value. When chloride content exceeds a certain level, I_{corr} denotes a sudden shift to greater values, indicating high corrosion rate. It should be noted that the pit growing rate (penetration depth rate) is assumed to be around 10 times higher than the average corrosion rate measured [21]. An I_{corr} of $0.1 \mu A/cm^2$ means that the pitting rate value could be higher than $1 \mu A/cm^2$, which indicates significant active corrosion. Also the CTV could be assumed to be from 0.05 to 0.06 mol/L according to I_{corr} evolution.

An abrupt change in topology of Nyquist plots of EIS can also be observed in Fig. 3. A typical Nyquist plot of steel immersed in simulated solution depicts a capacitive loop of depressed semicircles. As the concentration of chloride increases, the radius of the low-frequency semicircle gradually reduces, becoming from “linear” to “semicircular”.

An equivalent circuit shown in Fig. 4 was used to interpret EIS results, where R_s is the solution resistance and R_{ct} the charge

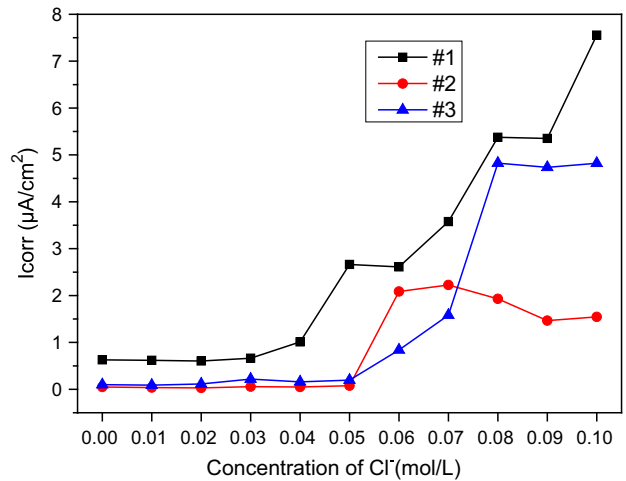


Fig. 2. Variations of I_{corr} of specimens with additions of chloride ions.

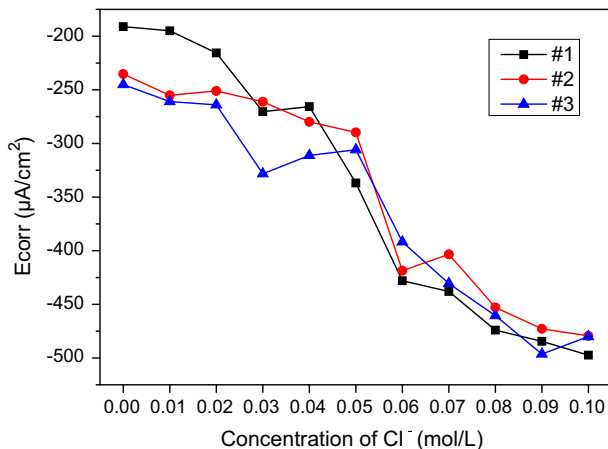


Fig. 1. Variations of E_{corr} of specimens with additions of chloride ions.

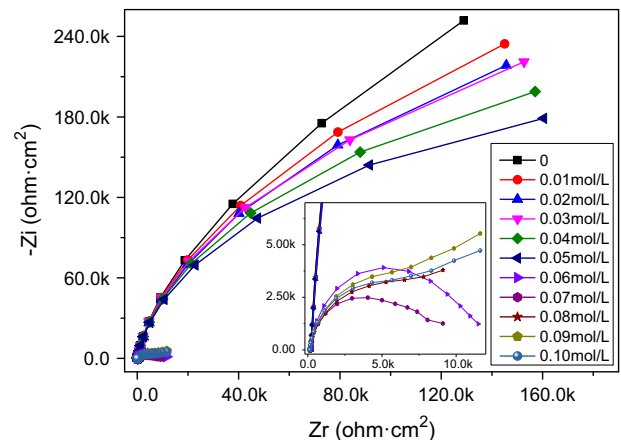


Fig. 3. Typical Nyquist plots of specimen with additions of chloride.

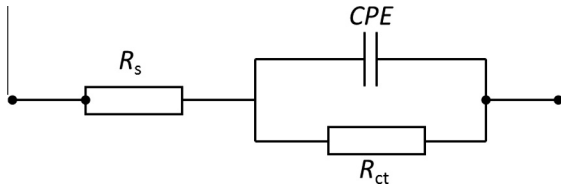


Fig. 4. Equivalent circuit of reinforcing steel immersed in simulated solutions.

transfer resistance. A greater R_{ct} value means more difficult for corrosion.

Constant phase element (CPE) represents the double-layer capacitance of the steel/electrolyte interface, and its impedance Z_{CPE} is defined as in Eq. (2).

$$Z_{CPE} = \frac{1}{Y_0(j\omega)^n} \quad (2)$$

where Y_0 is a parameter proportional to the double layer capacitance of pure capacitive electrodes, ω is the frequency in radians per second and n represents the deviated degree of the capacitance from the ideal condition, which ranges from 0 to 1. The CPE becomes a resistor when $n = 0$ and a capacitor when $n = 1$. In the concrete/steel system, passive film capacitance and double layer capacitance usually deviate from pure capacitance due to the dispersion effect, and the CPE is used instead of pure capacitance to represent the non-ideal frequency dependent capacitance in equivalent circuits. The behavior of CPE can be the result of the fractal nature or heterogeneity of electrode interface.

The fitting results of EIS data using the equivalent circuit are listed in Table 1. R_s value reduces steadily with additions of chloride, which means lower resistivity with more ions in electrolyte. R_{ct} reduces gradually as chloride content is increased. When the chloride content reached the CTV, between 0.05 and 0.06 mol/L in this case, R_{ct} declined rapidly by orders of magnitude due to the breakdown of passive film of steels. It can be seen that the CTVs concluded from E_{corr} , I_{corr} and EIS are in good consistency.

Additionally, when the steel electrode is immersed in simulated pore solution, a double electric layer or passive film tends to be established, making the solution/steel interface act more as pure capacitance and therefore the value of n is close to 1. Under chloride attack, passive film gradually breaks down, resulting in higher value of Y_0 and lower value of n .

3.2. Corrosion behavior in sulphate ions contaminated condition

Steel specimens labeled as #4, #5 and #6 exposed to sulphate ions attack show similar trend in E_{corr} compared to those in chloride contaminated conditions as can be seen in Fig. 5. With increasing sulphate ions, the E_{corr} levels off until a certain content of sulphate is added and a sharp decline in E_{corr} occurs. Compara-

Table 1
Fitting results of equivalent circuit for steel with different chloride contents.

Chloride content (mol/L)	R_s (Ω cm ²)	CPE		R_{ct} (Ω cm ²)
		$Y_0/10^{-5}$ (S cm ⁻² s ⁿ)	n	
0.00	211.6	3.67	0.9296	724,400
0.01	201.4	3.65	0.9255	591,200
0.02	187.3	3.72	0.9254	537,700
0.03	175.1	3.66	0.9299	527,800
0.04	163.6	3.70	0.9306	451,200
0.05	158.1	3.71	0.9305	391,700
0.06	142.6	6.15	0.8670	10,740
0.07	132.1	7.40	0.8325	7887
0.08	121.1	19.24	0.7949	9924
0.09	111.3	12.54	0.7979	10,460
0.10	98.31	12.32	0.8029	11,070

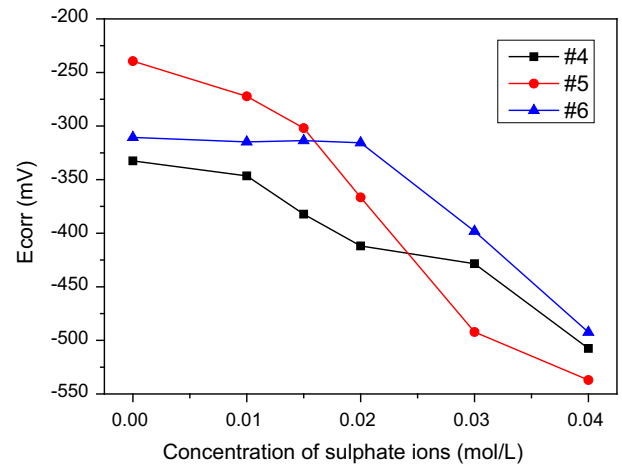


Fig. 5. Variations of E_{corr} of specimens with additions of sulphate ions.

ble to chloride threshold value, a sulphate threshold value of 0.02 mol/L can be inferred from this work. It is believed that the modification of the original iron oxide film to ferric sulphate film which was less protective caused the corrosion of steels subjected to sulphate ions [22,23]. It has been identified that sulphate shows a lower threshold value compared to chloride.

Likewise, a sudden shift in I_{corr} is shown in Fig. 6 when content of sulphate ions comes to threshold value. In the early stage, corrosion rate maintains low speed. When it exceeds the sulphate threshold content, pitting corrosion develops fast, leading to higher I_{corr} . It is notable that the initial I_{corr} of 4# sample are relatively higher than other samples probably due to inhomogeneity in local areas on the steel surface.

Typical Nyquist plots of specimen with increasing additions of sulphate ions are shown in Fig. 7. The capacitive loop in low frequency presents an obvious compressing trend between 0.02 and 0.03 mol/L of sulphate ions. Fitting data of EIS using equivalent circuit are listed in Table 2. The R_{ct} decreases by one order of magnitude when sulphate content changes from 0.02 to 0.03 mol/L.

3.3. Corrosion behavior in composite chloride-sulphate contaminated condition

In this part, pre-passivated steel specimens are exposed to chloride contaminated condition containing 0.6 mol/L of NaCl (3.5% by

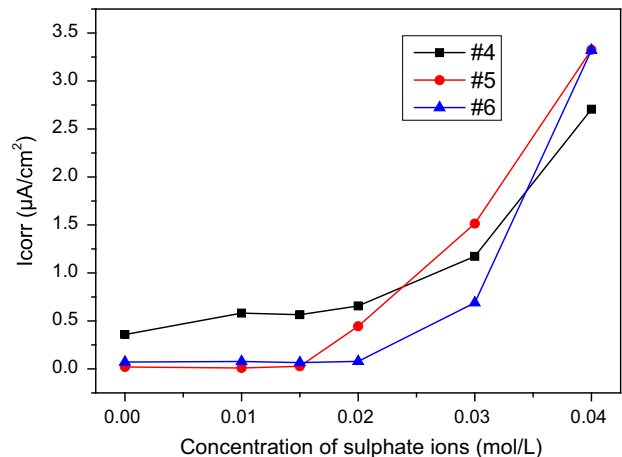


Fig. 6. Variations of I_{corr} of specimens with additions of sulphate ions.

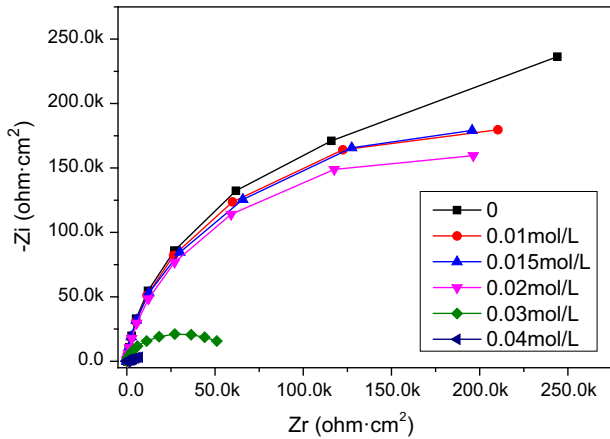


Fig. 7. Typical Nyquist plots of specimen with additions of sulphate ions.

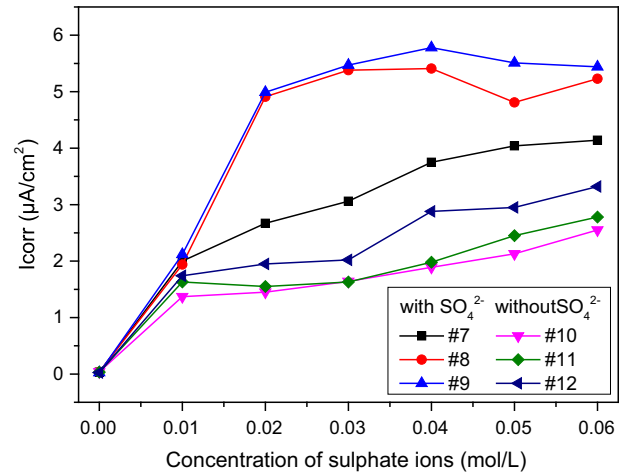


Fig. 9. Variations of I_{corr} of specimens subjected to chloride with and without sulphate attack.

Table 2
Fitting data of equivalent circuit for steel with additions of sulphate ions.

Sulphate content (mol/L)	R_s ($\Omega \text{ cm}^2$)	CPE		R_{ct} ($\Omega \text{ cm}^2$)
		$Y_0/10^{-5}$ ($S \text{ cm}^{-2} \text{ s}^{-1}$)	n	
0.00	232.6	3.041	0.9548	462,600
0.01	223	3.177	0.9529	381,900
0.015	173.7	3.111	0.9564	371,400
0.02	270.4	3.277	0.9428	346,000
0.03	146.3	4.288	0.9031	52,990
0.04	123.6	12.99	0.7004	6689

weight) to simulate marine service environment. Then sample #7, #8 and #9 were added with fixed concentration of chloride and 0.01 mol/L sulphate ions and were tested after 1d while sample #10, #11 and #12 are exposed to fixed concentration of chloride only.

Fig. 8 depicts the evolution of E_{corr} of all specimens. It can be seen that E_{corr} of all samples has gone below -500 mV after 24 h of exposure to 3.5% of NaCl. With or without further sulphate additions, E_{corr} of all samples remain steady between -500 and -600 mV . However, samples with sulphate attack show marked difference in I_{corr} as is shown in Fig. 9. Sulphate ions

added stepwise results in even higher I_{corr} than that without sulphate addition. High corrosion current density indicates fast pitting or general corrosion speed. From the results of this study, the concomitant presence of chloride and sulphate ions led to higher corrosion current density, which indicated severer corrosion of steel in simulated concrete pore solution. However, the precise mechanism through which sulphate ions influence the reinforcement corrosion is not well understood. It is inferred that a porous and non-passivating corrosion product layer formed by sulphate ions allows corrosion process to continue undisturbed. However, other researchers [24] attributed the comparative increase in corrosion rates to higher conductivity stemming from concentrated sulphate.

Typical Nyquist plots of specimen subjected to fixed concentration of chloride and varying concentrations of sulphate are shown in Fig. 10. The low-frequency arc reveals a dramatic change when chloride and sulphate are added. With subsequent dosage of sulphate ions, the compressing trend of capacitive semicircle continues. An obvious change of fitted R_{ct} can be found in Table 3. The R_{ct} decreased from 8.336×10^5 to 1.157×10^4 when fixed concentration of chloride and 0.01 mol/L sulphate ions are added and keeps reducing with more sulphate ions added.

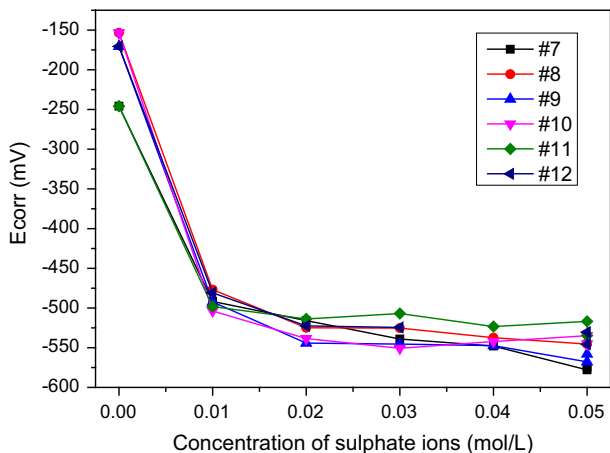


Fig. 8. Variations of E_{corr} of specimens subjected to chloride with and without sulphate attack.

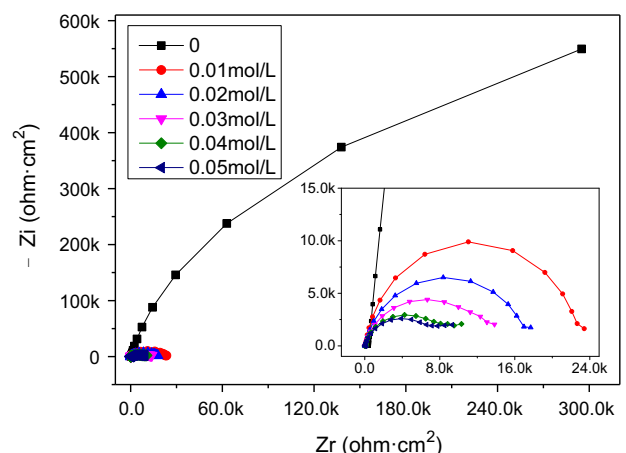


Fig. 10. Typical Nyquist plots of specimens subjected to fixed chloride concentration and varying sulphate concentrations.

Table 3

Fitted data of equivalent circuit for steel subjected to fixed chloride concentration and varying sulphate concentrations.

Sulphate content (mol/L)	Rs ($\Omega \text{ cm}^2$)	CPE		Rct ($\Omega \text{ cm}^2$)
		$Y_0/10^{-5}$ ($\text{S cm}^{-2} \text{ s}^{-1}$)	n	
0.00	207.4	3.724	0.9303	833,600
0.01	34.04	5.512	0.9034	11,570
0.02	33.81	7.075	0.8645	8540
0.03	32.85	8.685	0.8276	6554
0.04	31.11	9.472	0.8130	4741
0.05	32.08	10.430	0.7998	4274

4. Conclusion

Corrosion behavior and chloride threshold value of steels subjected to chloride and/or sulphate ions have been investigated in simulated concrete pore solution in this work. Electrochemical measurements of OCP, LP and EIS are utilized in combination to monitor corrosion evolution. Physical experiments were carried out not only to provide useful guidance and reference for specialists and engineers, but also to cast light upon likely corrosion mechanism when both chloride and sulphate are present. The following conclusions have been obtained:

- (1) A good correlation between OCP, LP and the EIS measurement has been found in monitoring corrosion behavior of steels. Determination of corrosion onset is suggested to use these non-destructive methods in combination. Ecorr, Icorr and Rct value have shown dramatic shift when aggressive ions reaches the threshold value.
- (2) The CTV of steels submitted to chloride ions obtained in this work is between 0.05 and 0.06 mol/L, whereas the corrosion threshold content of sulphate ions ranges from 0.02 to 0.03 mol/L. Lower threshold content means sulphate presents more aggressive corrosion risk to steel, partially due to the porous and non-passivating corrosion product induced by sulphate.
- (3) The concomitant presence of chloride and sulphate ions leads to higher corrosion current density than specimens exposed to chloride ions at corresponding concentration, which indicated corrosion rate of steel specimens accelerates when both chloride and sulphate are in presence in simulated concrete pore solution.

Acknowledgment

Authors gratefully acknowledge the financial support from 973 Program (2015CB655102) and Natural Science Foundation of China (51378116).

References

- [1] C. Arya, N.R. Buenfeld, J.B. Newman, Assessment of simple methods of determining the free chloride ion content of cement paste, *Cem. Concr. Res.* 17 (1987) 907–918.
- [2] G. Blanco, A. Bautista, H. Takenouti, EIS study of passivation of austenitic and duplex stainless steels reinforcements in simulated pore solutions, *Cem. Concr. Compos.* 28 (2006) 212–219.
- [3] P. Ghods, O.B. Isgor, G.A. McRae, G.P. Gu, Electrochemical investigation of chloride induced depassivation of black steel rebar under simulated service conditions, *Corros. Sci.* 52 (2010) 1649–1659.
- [4] A.M. Vaysburd, P.H. Emmons, How to make today's repairs durable for tomorrow-corrosion protection in concrete repair, *Constr. Build. Mater.* 14 (2000) 189–197.
- [5] J. Hu, D.A. Koleva, J.H.W. De Wit, H. Kolev, K. Van Breugel, Corrosion performance of carbon steel in simulated pore solution in the presence of micelles, *J. Electrochem. Soc.* 158 (2011) 76–87.
- [6] Z. Liu, Y. Zhang, Q. Jiang, Continuous tracking of the relationship between resistivity and pore structure of cement pastes, *Constr. Build. Mater.* 53 (2014) 26–31.
- [7] Z. Liu, Y. Zhang, Q. Jiang, et al., Solid phases percolation and capillary pores depercolation in hydrating cement pastes, *J. Mater. Civ. Eng.* 26 (2013). 04014090.
- [8] S.E. Hussain, Rasheeduzzafar, A. Al-Musallam, A.S. Al-Gahtani, Factors affecting threshold chloride for reinforcement corrosion in concrete, *Cem. Concr. Res.* 25 (1995) 1543–1555.
- [9] M. Thomas, Chloride thresholds in marine concrete, *Cem. Concr. Res.* 26 (1996) 513–519.
- [10] L.T. Mammoliti, L.C. Brown, C.M. Hansson, B.B. Hope, The influence of surface finish of reinforcing steel and pH of the test solution on the chloride threshold concentration for corrosion initiation in synthetic pore solutions, *Cem. Concr. Res.* 26 (1996) 545–550.
- [11] M. Manera, O. Vennesland, L. Bertolini, Chloride threshold for rebar corrosion in concrete with addition of silica fume, *Corros. Sci.* 50 (2008) 554–560.
- [12] U. Angst, B. Elsener, C.K. Larsen, Ø. Vennesland, Critical chloride content in reinforced concrete – a review, *Cem. Concr. Res.* 39 (2009) 1122–1138.
- [13] Z.Q. Jin, W. Sun, Y.S. Zhang, J.Y. Jiang, J.Z. Lai, Interaction between sulfate and chloride solution attack of concretes with and without fly ash, *Cem. Concr. Res.* 37 (2007) 1223–1232.
- [14] T.H. Wee, A.K. Suryavanshi, S.F. Wong, A.K.M. Anisur Rahman, Sulfate resistance of concrete containing mineral admixtures, *ACI Mater. J.* 97 (2000) 536–549.
- [15] M. Santhanam, M.D. Cohen, J. Olek, Mechanism of sulfate attack: a fresh look Part 1. Summary of experimental results, *Cem. Concr. Res.* 32 (2002) 915–921.
- [16] D. Izquierdo, C. Alonso, C. Andrade, M. Castellote, Potentiostatic determination of chloride threshold values for rebar depassivation: experimental and statistical study, *Electrochim. Acta* 49 (2004) 2731–2739.
- [17] M. Moren, W. Morris, M.G. Alvarez, et al., Corrosion of reinforcing steel in simulated concrete pore solutions: effect of carbonation and chloride content, *Corros. Sci.* 46 (2004) 2681–2699.
- [18] L. Jiang, G. Huang, J. Xu, et al., Influence of chloride salt type on threshold level of reinforcement corrosion in simulated concrete pore solutions, *Constr. Build. Mater.* 30 (2012) 516–521.
- [19] M. Stern, A.L. Geary, Electrochemical polarization I A theoretical analysis of the shape of polarization curves, *J. Electrochem. Soc.* 104 (1957) 56–63.
- [20] C. Andrade, J.A. Gonzalez, Quantitative measurements of corrosion rate of reinforcing steels embedded in concrete using polarisation resistance measurements, *Mater. Corros.* 29 (1978) 515–519.
- [21] C. Alonso, C. Andrade, M. Castellote, P. Castro, Chloride threshold values to depassivate reinforcing bars embedded in a standardized OPC mortar, *Cem. Concr. Res.* 30 (2000) 1047–1055.
- [22] A.J. Al Teyyib, S.K. Somuah, J.K. Booh, P. Leblac, A.J. Al Mana, Laboratory study on the effect of sulfate ions on rebar corrosion, *Cem. Concr. Res.* 18 (1988) 249–256.
- [23] N. Mursalo, M. Tullmin, F.P. Robinson, The Corrosion behaviour of mild steel, 3CR12, and AISI type 316L in synthetic mine waters, *J. South Afr. Inst. Min. Metall.* 88 (1988) 249–256.
- [24] G. Singh, A survey of corrosivity of underground mine waters from Indian coal mines, *Int. J. Mine Water* 5 (2006) 21–32.